

# FLUORESCENCE TOMOGRAPHY: RECONSTRUCTION BY ITERATIVE METHODS

Eduardo X. Miqueles and Alvaro R. De Pierro

Applied Mathematics Department, State University of Campinas, Brazil

## ABSTRACT

X-Ray fluorescence computed tomography (XFCT) aims at reconstructing fluorescence density from emission data given the measured X-Ray attenuation. In this paper, inspired by emission tomography (ECT) reconstruction literature, we propose and compare different reconstruction methods for XFCT, based on iteratively inverting the generalized attenuated Radon transform. We compare the different approaches using simulated and real data as well.

**Index Terms**— fluorescence tomography, emission tomography, attenuation, generalized Radon transform

## 1. INTRODUCTION

X-Ray fluorescence computed tomography (XFCT) is a relatively new synchrotron based imaging modality that can be seen as a stimulated emission tomography [2]. In XFCT a sample is irradiated with high intensity monochromatic synchrotron X-rays with energy greater than the K-shell binding energy of the elements of interest. This stimulates fluorescence emission, at certain characteristic energies, isotropically distributed, which are detected by a detector placed parallel to the direction of the incident beam [7]. Part of the emission is absorbed by the sample, so, correction for attenuation is essential to obtain qualitative better results. Mapping fluorescence emission density distributions could have many important biomedical applications [9].

A continuous mathematical model for XFCT is given by the generalized attenuated Radon Transform [6]; that is, if  $\theta \in [0, 2\pi]$  and  $t \in [-1, 1]$  are the parameters defining the line where emission occurred, and  $d(t, \theta)$  is the number of detected emissions coming from some point on that line, we have that, for the emission density  $f$ , defined in the unit disc  $\Omega$ :

$$d(t, \theta) = \mathcal{R}_W f(t, \theta) = \int_{\mathbf{x} \cdot \xi = t} W(\mathbf{x}, \theta) f(\mathbf{x}) d\mathbf{x}$$

where  $\xi = (\cos \theta, \sin \theta)$ ,  $\xi^\perp = (-\sin \theta, \cos \theta)$  and

$$W(\mathbf{x}, \theta) = e^{-D\lambda(\mathbf{x}, \theta + \pi)} \int_{\gamma_1}^{\gamma_2} e^{-D\mu(\mathbf{x}, \theta + \gamma)} d\gamma,$$

First author supported by FAPESP grant No 06/00356-6 and second author by FAPESP grant No 2002/07153-2 and CNPq grants No 476825/2006-0 and 304820/2006-7

is the weight function and the operator  $D$  is defined by

$$D\mu(\mathbf{x}, \theta) = \int_0^\infty \mu(\mathbf{x} + q\xi^\perp) dq,$$

also known as the *divergent beam transform*. The fluorescence radiation leaves the object within the angle range  $[\gamma_1, \gamma_2]$  at each emission point. Here,  $\mu$  stands for the fluorescence attenuation and  $\lambda$  for the transmission one. Therefore, in a continuous setting, the mathematical problem consists of approximately inverting the operator  $\mathcal{R}_W$ , for known  $\lambda$  and estimated  $\mu$ .

It is easy to prove that the adjoint operator of  $\mathcal{R}_W$  is defined by

$$\mathcal{B}_W d(\mathbf{x}) = \int_0^{2\pi} W(\mathbf{x}, \theta) d(\mathbf{x} \cdot \xi, \theta) d\theta$$

with  $d = d(t, \theta)$ . We call  $\mathcal{B}_W$  the attenuated backprojection operator. If  $\mu = \lambda = 0$ , then  $\mathcal{R}_W = \mathcal{R}$  is the classic Radon Transform and  $\mathcal{B}_W = \mathcal{B}$  the standard backprojection operator.

In the next two Sections we present the methods. Section 4 describes the numerical experiments comparing them with simulated and real data and Section 5 presents some conclusions.

## 2. ITERATIVE INVERSION OF THE ATTENUATED TRANSFORM

For given  $\lambda$  and  $\mu = 0$ , working in emission tomography, Chang [3] suggested the approximation

$$f_c(\mathbf{x}) = \frac{1}{2\pi} \frac{\mathcal{R}^{-1}\{d\}(\mathbf{x})}{a(\mathbf{x})}$$

as an estimate of the density  $f$ , where  $a = a(\mathbf{x})$  corresponds to the correction

$$a(\mathbf{x}) = \frac{1}{2\pi} \int_0^{2\pi} W(\mathbf{x}, \theta) d\theta.$$

Independently, Hogan *et al* [5], after an appropriate discretization, obtained the same formula as Chang, that is the one currently being used in fluorescence tomography, when fluorescence attenuation is known.

Inspired by work by Kunyansky [6] we observed that Chang-Hogan's method is nothing but the first iteration of

an iterative method. Each iteration consists of considering the inverse Radon Transform  $\mathcal{R}^{-1}$ , weighted by the factor  $\frac{1}{a}$ , very easy to calculate, as an approximation of the inverse of the attenuated Radon Transform,  $\mathcal{R}_W^{-1}$ ; then a correction by the residual gives the next iterate. That is, the sequence is defined by

$$f^{(k+1)} = f^{(k)} + \alpha_k e^{(k)} \quad (1)$$

where we have introduced the positive relaxation factor  $\alpha_k$  and

$$e^{(k)} = \frac{\mathcal{R}^{-1}(d - \mathcal{R}_W f^{(k)})}{a}$$

So, the first iteration, with  $f^{(0)} = 0$  and  $\alpha_k = 1 \forall k$  gives Chang-Hogan's correction.  $\alpha_k$  is a relaxation factor that for high attenuation values could be used to accelerate the method when greater than one.

### 3. THE EM ALGORITHM

Together with the "continuous" inversion, and following [4] we will compare the results with the standard EM algorithm for the problem. The EM algorithm is defined by the iteration (for known  $\{\mu, \lambda\}$ ):

$$f^{(k+1)}(\mathbf{x}) = f^{(k)}(\mathbf{x}) \frac{\mathcal{B}_W d^{(k)}(\mathbf{x})}{\mathcal{B}_W e(\mathbf{x})} \quad (2)$$

where  $e(t, \theta) = 1, \forall (t, \theta) \in [0, 2\pi] \times [-1, 1]$ , and

$$d^{(k)}(t, \theta) = \frac{d(t, \theta)}{\mathcal{R}_W f^{(k)}(t, \theta)}.$$

### 4. NUMERICAL EXPERIMENTS

We performed several numerical experiments with simulated and real data, that are summarized next. In order to compare algorithms (1) and (2),  $f^{(0)}|_{\Omega} = \epsilon$  was chosen as the initial point, since the EM algorithm cannot converge starting from the null image. For fluorescence experiments applied in soft tissues, the density function  $f$  usually has a very low order of magnitude, say  $f(\mathbf{x}) \approx 10^{-6}$ , so, for our numerical experiments, we used  $\epsilon = 10^{-7}$ .

#### Simulated Data

The phantom for these simulations follows Brunetti *et al's* [1], but with a modified geometry, in order to test the algorithms performance for borders identification. The 512x512 pixels images of  $f$  and  $\lambda$  are shown in figure 1. In this example,  $\mu = 2\lambda$ . 150 views (uniform angles in  $[0, 2\pi]$ ) and 150 rays for each view were used. Figure 2 shows the reconstructions by both algorithms using  $\mu \neq \lambda$ , first and fourth iterations. Figures 3 and 4 are the reconstructions for the line  $x = -0.30$  using  $\mu \neq \lambda$  and  $\mu = \lambda$ . Figure 5 shows the

reconstructions with  $\mu = \lambda$  for each algorithm after 100 iterations. It is clear the improvement obtained when increasing the number of iterations. A higher likelihood value is attained very fast by Alg (1).

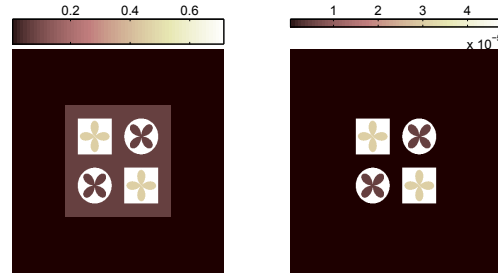


**Fig. 1.** Phantom, 512x512 pixels. Left: Transmission attenuation. Right: Density emission.

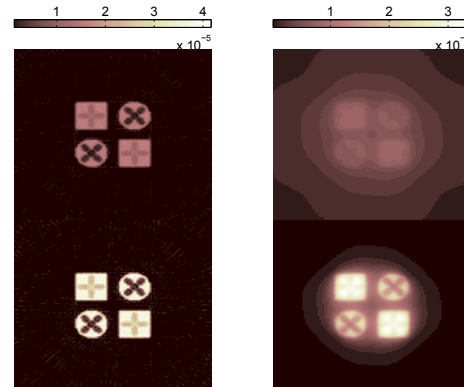


**Fig. 2.** Reconstructions with  $\mu \neq \lambda$ . Left (top): one iteration of 1. Left (bottom): four iterations of 1. Right: same for algorithm 2.

#### Real Data

We performed reconstructions from experimental data from samples of breast tissue to observe details of ductal carcinoma structures. This was done by reconstructing the distributions of Fe, Cu and Zn. The data was obtained from a system that was set up in a high-resolution diffraction beam line at the Brazilian Synchrotron Light Source (LNLS) in Campinas, São Paulo. The fluorescence attenuation map  $\mu$  was not available a priori, so  $\mu = \lambda$  was used as an approximation. The results are shown in Figures 6,7 and 8. As for the simulated data, that is, with known geometry, contrast clearly increases with the number of iterations.

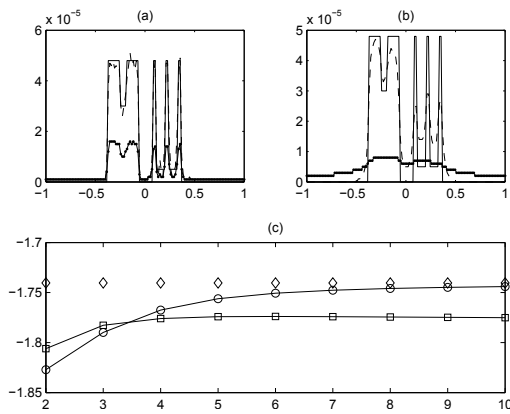


**Fig. 3.** Graphics along the line  $x = -0.30$  for  $\mu \neq \lambda$  for the phantom. The continuous line represents the phantom, the dotted line ten iterations, the pointed line one iteration. (a) For Alg (1) (b) For Alg (2) (c) Loglikelihood function for the ten first iterations. Alg (1); circles, Alg (2); squares, Ideal values: diamonds.

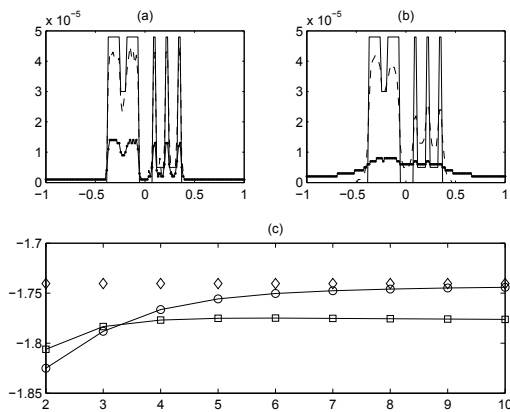


**Fig. 4.** Same as Figure 3 for  $\mu = \lambda$ .

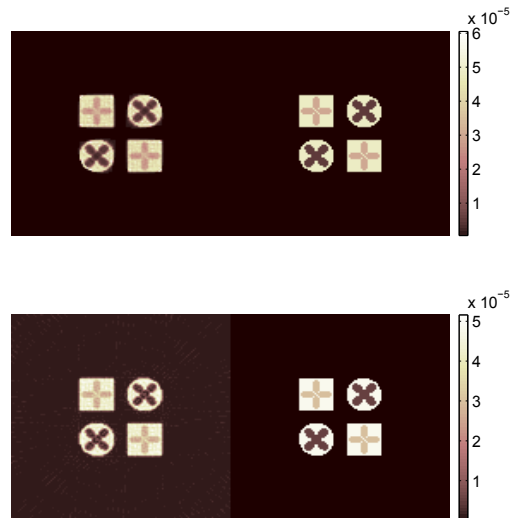


**Fig. 5.** Reconstructions for  $\mu = \lambda$  after 100 iterations for the discontinuous phantom. Top: Alg (2) vs. original; bottom: Alg (1) vs. original.

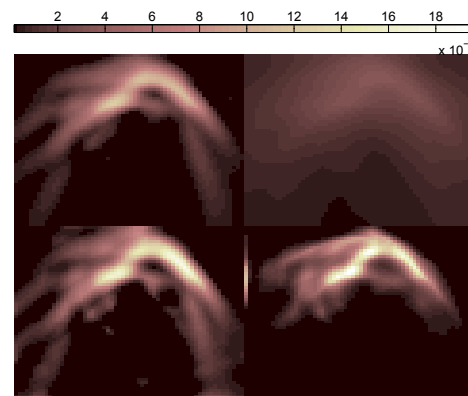


**Fig. 6.** Reconstruction of Fe density using  $\mu = \lambda$ . The first column represents iterations one and fifty for Alg(1), the second for Alg(2).

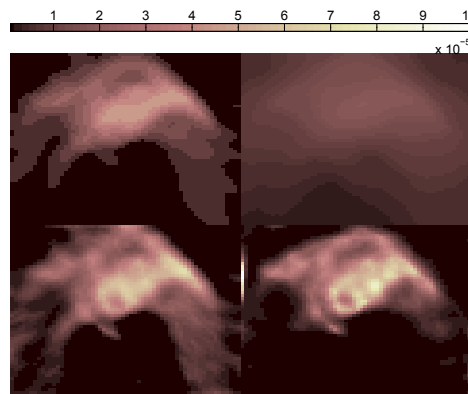


**Fig. 7.** Same as Figure 6 for Cu.

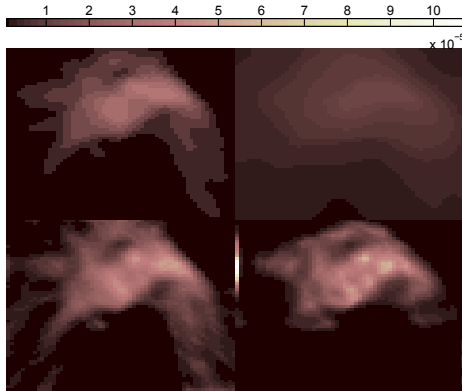


**Fig. 8.** Same as Figure 6 for Zn.

## 5. CONCLUSIONS

In the current XFCT literature the main inversion method has been Hogan *et al*'s. In this article we show that the method is just the first iterate of a more general iterative method based on the weighted inversion of the Radon Transform. Our experiments show that the quality of the images could be very much improved when several iterations are used. From our simulations and experiments with real data, we can see that this improvement is also valid when the unknown fluorescence attenuation is estimated by the transmission attenuation map. We are working now in two directions: the fast retrieval of the fluorescence attenuation from the emission data only and the reconstruction from smaller data sets, aiming at reducing the experimental time. Also, we are comparing our approach with the one proposed in [7], using a phantom with known geometry to verify the reconstruction accuracy.

## 6. ACKNOWLEDGMENTS

We are very grateful for the support of the researchers of the Nuclear Instrumentation Laboratory (Federal University of Rio de Janeiro), Brazil, and the Brazilian Synchrotron Light Laboratory (LNLS).

## 7. REFERENCES

- [1] A.Brunetti, B.Golosio, *Software for X-ray fluorescence and scattering tomographic reconstruction*, Computer Physics Communications, vol.141, pp.412-425, 2001.
- [2] R.Cesareo, S.Mascarenhas, *A new tomographic device based on the detection of fluorescent x-rays*, Nucl. Instrum. Methods A, 277, pp. 667-672, 1989.
- [3] L.T.Chang, *A Method for Attenuation Correction in Radionuclide Computed Tomography*, IEEE Trans. Nucl. Science, NS-25, No.1, pp.638-648, 1978.
- [4] G.Friedmann Rust, J.Weigelt, *X-ray fluorescent computer tomography with synchrotron radiation*, IEEE Trans. Nucl. Science, vol.45, No. 1, 1998.
- [5] J.P.Hogan, R.A.Gonsalves, A.S.Krieger, *Fluorescent Computer tomography: a model for correction of X-Ray absorption*, IEEE Trans. Nucl. Science, vol 38, No.6, 1991.
- [6] L.A.Kunyansky, *Generalized and attenuated Radon transforms: restorative approach to the numerical inversion*, Inverse Problems, 8, pp. 809-819, 1992.
- [7] P.La Rivière, P.Vargas, *Monotonic Penalized-likelihood image reconstruction for X-ray fluorescence computed tomography*, IEEE Trans. Med. Imaging, vol.25, No.9, 2006.
- [8] P.La Rivière, *Approximate analytic reconstruction in X-ray fluorescence computed tomography*, Phys.Med.Biol., 49, pp.2391-2406, 2004.
- [9] H.S.Rocha, G.R.Pereira, M.J.Anjos, P.Faria, G.Kellerman, C.A.Pérez, G.Tirao, I.Mazzaro, C.Giles, R.T.Lopes, *Diffraction enhanced imaging and x-ray fluorescence microtomography for analysing biological samples*, X-Ray Spectrometry, vol.36, pp.247-253, 2007.